

A Phononic Crystal Strip with Lowering and Extending Band Gaps

Thi Dep Ha¹, JingFu Bao²

School of Electronic Engineering^{1,2}, University of Electronic Science and Technology of China, Chengdu 611731, China^{1,2}

*Faculty of Electronic Technology¹, Industrial University of Ho Chi Minh City, Ho Chi Minh City, Vietnam¹
Email: hathidep@yahoo.com¹, baojingfu@uestc.edu.cn²*

Abstract-The band gap width and location of phononic crystal (PnC) in band structure demonstrate its effectiveness on preventing leaked energy from MEMS resonator body into substrate through support tethers. In this paper, we propose a novel phononic crystal strip which is composed of horizontal and vertical stubs made of tungsten on silicon host to reduce the side dimensions and lower and widen acoustic band gaps. Four types of material based stub arrangements investigated in our work are silicon stubs, metallic vertical stub, metallic horizontal stub and metallic stubs. We utilize the finite element method in COMSOL Multiphysics software (COMSOL) to analysis and simulate the proposed PnC strip. The simulation results show that the gaps of the proposed model obtain dominant widths and occupy very low frequency range in the band structure. The gap width and location can optimize through both horizontal and vertical stubs. Among these configuration, the gap number and density of the proposed PnC strip with metallic stubs are heaviest and closest.

Index Terms- phononic crystals; band gap; band structure.

1. THE MAIN TEXT

The acoustic wave propagation in phononic crystal (PnC), which are composed of periodic structures with scattering inclusions in solid host, has attracted considerable attention in recent years[1, 2]. One of key characteristics of the PnC structures is band gap map (i.e. band structure, band gap diagram)[1] which shows the width and position of the gaps in certain wave frequency ranges. A band gap is the frequency range in which the acoustic waves cannot pass into the structures[2, 3]. The wider the band gap, the higher the effectiveness of acoustic wave propagation isolation. Thus, the PnC operate as acoustic wave barriers. Several researches have been reported for PnC strip (1D)[1, 4], PnC slab (2D)[3] and PnC pillar (3D)[5]. In addition, geometrical parameters of the PnC structures also effect on form factor of PnC based devices. For MEMS support tether applications, PnC strip exhibits great advantages such as simple, space saving compared to others[1]. To the best of our knowledge, there is no report on horizontal and vertical stub combination as well as the embedding of metallic stubs on silicon host for the PnC strip to optimize and lower band gap formation up to now.

This paper proposes a novel PnC strip configuration which is combined horizontal and vertical stubs in silicon background to obtain significantly wide and low band gaps and small form factor (i.e. reducing the side dimensions) for MEMS applications. The structure is designed for four types

of stubs with different materials including silicon, metallic horizontal, metallic vertical and metallic stubs. We also investigate the sensitivity of the band structure to the geometrical parameters (e.g. the length of the horizontal and vertical stubs) of the proposed model and compare with conventional ones. The simulations and their result processing are performed via COMSOL Multiphysics (the software for finite element (FE) analysis) and MATLAB.

2. MODELING

Figure 1 shows the schematic diagram of the proposed PnC trip. Each unit cell is composed of horizontal and vertical double-sided stubs on silicon background as illustrated in Fig. 1a. As this figure shown, these stubs are made of silicon (indicated by gray bars) or metal (indicated by green bars), namely tungsten (W), and arranged into four schemes. Geometrical parameters for each cell are as follow: the lattice constant a of 28 μm , the lattice width W_a of 6 μm , the lattice thickness h of 3 μm , the vertical stub length L_v of 22 μm , the horizontal stub length L_h of 22 μm and the horizontal stub width W_h of 6 μm . The PnC strip model with three unit cells is shown in Fig. 1b.

Materials used for the PnC structure in this paper consist of silicon and tungsten. Silicon has elastic constants $c_{11} = 165.7 \times 10^9 \text{ Pa}$, $c_{12} = 63.9 \times 10^9 \text{ Pa}$, $c_{44} = 79.55 \times 10^9 \text{ Pa}$, $\rho = 2330 \text{ kg/m}^3$ [6]. Tungsten is used for the stubs and has $c_{11} = 52.9 \times 10^{10} \text{ Pa}$, $c_{12} = 20.918 \times 10^{10} \text{ Pa}$, $c_{44} = 16.19 \times 10^{10} \text{ Pa}$ and $\rho = 19361.5 \text{ kg/m}^3$ [7].

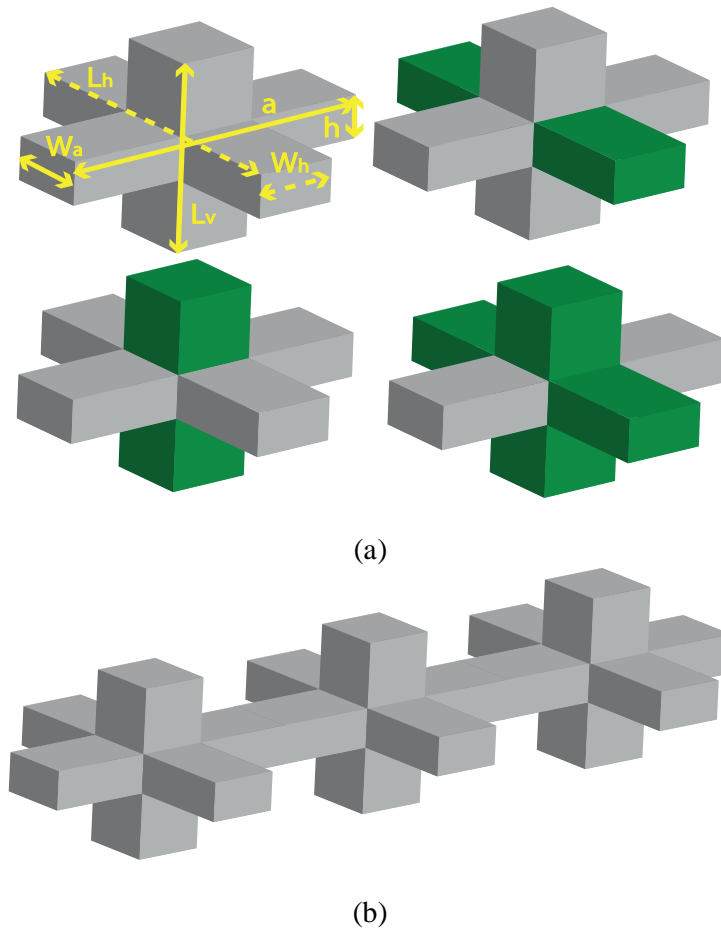


Fig. 1. Three dimensional schematic of the proposed PnC strip configuration (a) four types of unit cells (the green indicated W, the grey indicated silicon), (b) the periodical structure with three unit cells.

In order to obtain dispersion curves and eigen modes in the proposed PnC model, the finite element simulation tool, namely COMSOL Multiphysics, is used in our work. The band gap map is then calculated from these simulation results using MATLAB. Due to the periodicity of the PnC structure, we perform the simulations for a unit cell and apply the Bloch Floquet boundary condition[8] to the simulated unit cell to repeat this structure.

3. SIMULATION RESULTS AND DISCUSSION

3.1. The dispersion curves and eigen modes

Using the given geometrical parameters in section 2 and FEM, the phononic dispersion curves, band gaps and eigen modes of the conventional and proposed PnC strips are calculated and plotted in Fig. 2.

Figure 2a-b shows the dispersion curves for the conventional PnC strips (i.e. the stubs are vertical or horizontal). As the figure shown, two gaps with significant width of the PnC strip with vertical stub occur in the 0 – 150 MHz and their values are 11.23 and 18.4 MHz (with lower gap boundary of 59.98 and 123.56 MHz, respectively) while the gaps of the counterpart with horizontal stub almost disappear in this frequency range and have four band gaps with the

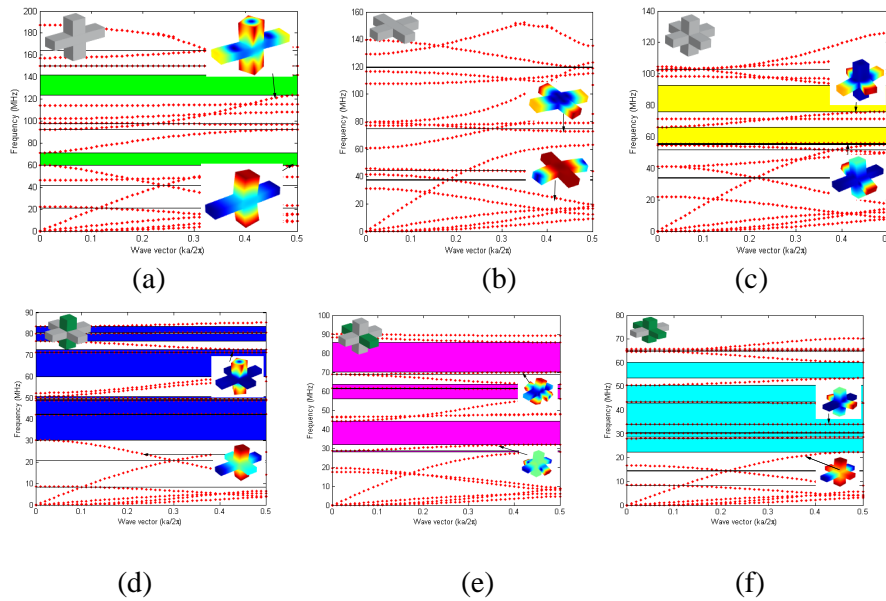


Fig. 2. Dispersion curves, band gaps and eigen modes of the (a) conventional PnC strip with vertical stub, (b) conventional PnC strip with horizontal stub, (c) proposed PnC strip with silicon stubs, (d) proposed PnC strip with metallic vertical stub, (e) proposed PnC strip with metallic horizontal stub, (f) proposed PnC strip with metallic stubs.

highest value of 0.41 MHz (with lower gap boundary of 37.41 MHz).

Figure 2c-f plots the dispersion curves and band gaps of the proposed PnC model with silicon (Fig. 2c), metallic vertical (Fig. 2d), metallic horizontal (Fig. 2e) and metallic stubs (Fig. 2f). The band gap number shown in Fig. 2c is five in the 0 - 140 MHz in which two large band gaps among these gaps are 10.2 and 16.63 MHz (corresponding with the lower gap boundary of 56.06 and 75.89 MHz). For metallic stubs, the wide gaps are 11.94, 6.35 and 11.43 (with lower gap boundary of 30.39, 42.48 and 59.92 MHz); 12.21, 5.3 and 15.83 (with lower gap boundary of 32.04, 56.02 and 70.01 MHz); 5.64, 1.74, 3.58, 8.81, 6.94 and 6.79 (with lower gap boundary of 22.51, 28.69, 30.55, 34.15, 43.62 and 53.51 MHz) corresponding with metallic vertical stub, metallic horizontal stub and metallic stubs. The eigen modes illustrated in these figures are obtained from the simulated results with wave vector k of 0.5.

3.2. The band gap diagram of the PnC strip with conventional stubs

To highlight the effectiveness of the proposed model on creating low and wide band gaps, we study the classical PnC strips with different parameters of the stub length as a background of comparison. These parameters are the same ones of the proposed

structure. The simulated and calculated results are shown in Fig. 3. It is clear from this figure that it is not easy to obtain the gaps in low frequencies. The band gaps are almost around the 100 - 150 MHz for both structures.

For the PnC strip with horizontal stub, the largest gap is 22.47 MHz (as shown in the magenta area of the graph) corresponding with the lower gap boundary of 92.64 MHz and stub length L_h of 18 μm . This gap is opened at 14 μm and closed at 20 μm . In the 43 - 54 MHz, the widest gap is 6.69 MHz (as shown in the blue area of the graph) for L_h of 28 μm .

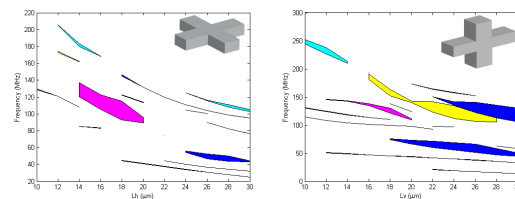


Fig. 3. Effect of the length of the stubs on the band structure of the PnC strip with conventional stubs (the left one is the PnC strip with horizontal stub, the right one is the PnC strip with vertical stub).

Studying the same geometrical dimensions for the PnC strip with vertical stub, we can observe that this type of stub can open gap more and lower than the horizontal stub. In detail, in the 51.74 - 66.6 MHz and L_v of 26 μm , the widest gap is 14.86 MHz (as shown in the lower blue area of the graph). Another value is 24.61 MHz (as shown in the upper blue area of the graph) in 105.39 - 130 MHz when L_v is 30 μm . Besides, increasing stub length makes these band gaps closer.

3.3. The band gap diagram of the proposed PnC strip versus the length of horizontal stub

To further understand the sensitivity of the band gap to the geometrical dimension as well as material made of the stubs, we firstly investigate the horizontal stub length variation of from 10 to 30 μm for four types of the stubs. The other parameters are kept as described in section 2. The first type shown in Fig. 4a is the PnC strip with silicon stubs. In this configuration, several band gaps are opened in the 0 - 150 MHz and

relatively large. Specifically, the gaps are around 40 - 70 MHz when the stub length L_h increases in the range of 20 to 30 μm . These gaps are shifted to higher frequencies (i.e. around 120 - 140 MHz) when L_h trends to decrease. The maximum gaps achieve 31.1 MHz at 113.9 MHz for L_h of 12 μm and 10.2 MHz at 56.1 MHz for L_h of 22 μm .

Figure 4b plots the band gap map of the second type with metallic vertical stub. One can see from this graph that the density of the gaps is heavy and approximately continuous on the gap map when the stub length varies from 10 to 30 μm . Moreover, these gaps are almost adjacent. This leads to the effectiveness and safety of the PnC structure on elastic wave stop better. For example, a band gap of 11.94 MHz exists in the 30.39 - 42.43 MHz and another gap of 6.37 MHz simultaneously occurs in the 42.46 - 48.83 MHz for L_h of 22 μm (indicated by yellow and blue areas in the figure). We can observe this phenomenon in the higher frequency range of 77.2 -

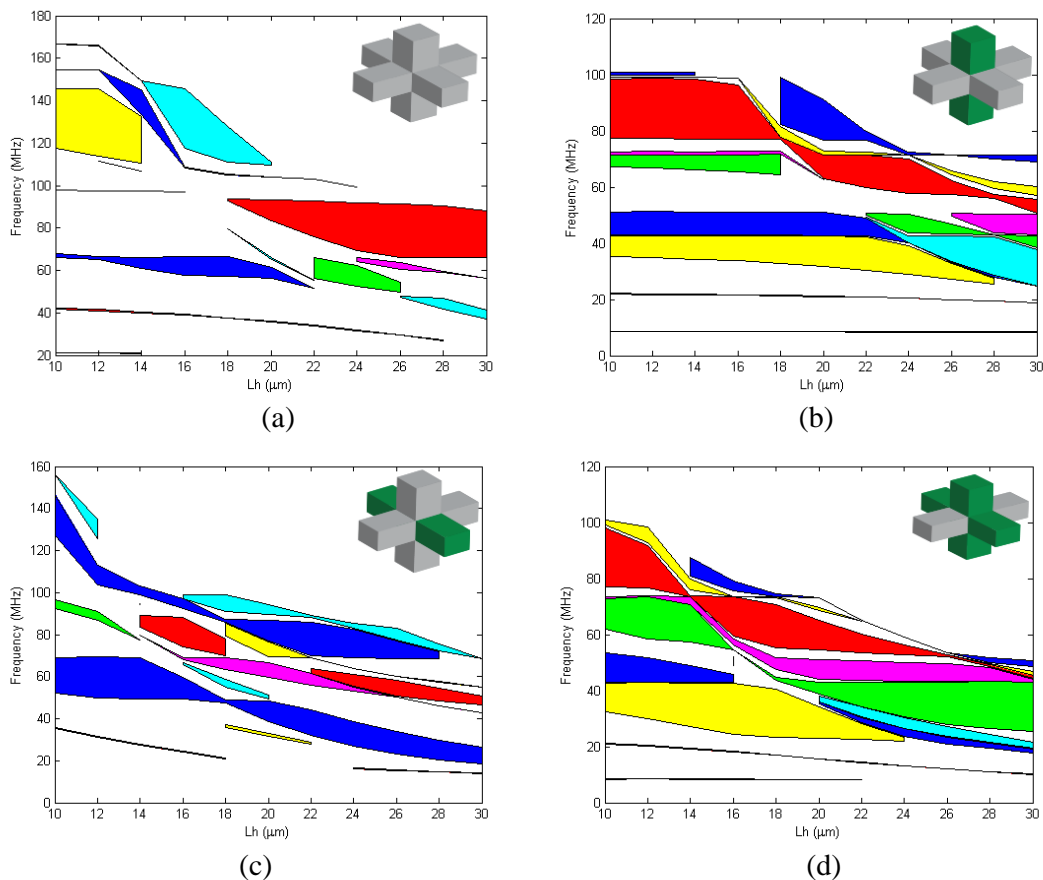


Fig. 4. Dependence of the band structure of the proposed PnC strip with (a) silicon stubs, (b) metallic vertical stub, (c) metallic horizontal stub, (d) metallic stubs on the horizontal stub length.

100.94 MHz and Lh of 10 μm as shown in the graph. Three gaps in this range are 21.35, 0.017 and 1.19 MHz in the 77.2 - 98.55, 99.1 - 99.12 and 99.75 - 100.94 MHz.

The band gap map of the third type with metallic horizontal stub is illustrated in figure 4c. As the figure shown, all band gaps are concentrated around 20 – 100 MHz and trend to move to lower frequencies when increasing the stub length. All gap widths in this type are dominant. Some band gaps almost continually appear. The band gap position can be obtained at around 20 MHz for Lh of 30 μm . Figure 4d graphed the fourth type of the PnC strip which combined metallic horizontal with vertical stubs. Compared with three other types of the stubs, this structure opens most band gaps in the 30 – 100 MHz. These gaps trend to shift to lower frequencies when the stub length Lh become larger. Similarly, the gap map shows that the appearance of the gaps is very close. This leads to that the width of the gap can become larger and is one of desirable characteristics in designing PnC strip.

3.4. The band gap diagram of the proposed PnC strip versus the length of vertical stub

In this section, we investigate the evolution of the band structure including the gap width and position as a function of the vertical stub length. This length is from 10 to 30 μm while keeping other geometrical parameters as discussed in section 2. The simulated and calculated results plotted in Fig. 5 are also performed for four types of the stubs as presented in 3.3.

Figure 5a shows the gap map of the whole silicon PnC strip. Most band gaps exist in the 60 – 120 MHz and are opened at Lh of 14 μm . The gaps are larger in the stub length range of 20 - 22 μm . All band gaps are shifted to low frequency range when the stub become longer. This is contrary to the gap map of the same structure with horizontal stub length variation where most gaps is opened and obtain large width when reducing or increasing the length out of range of 20 – 22 μm . For example, the highest gap is 20.25 MHz and its lower gap boundary is 76.49 MHz for Lv of 20

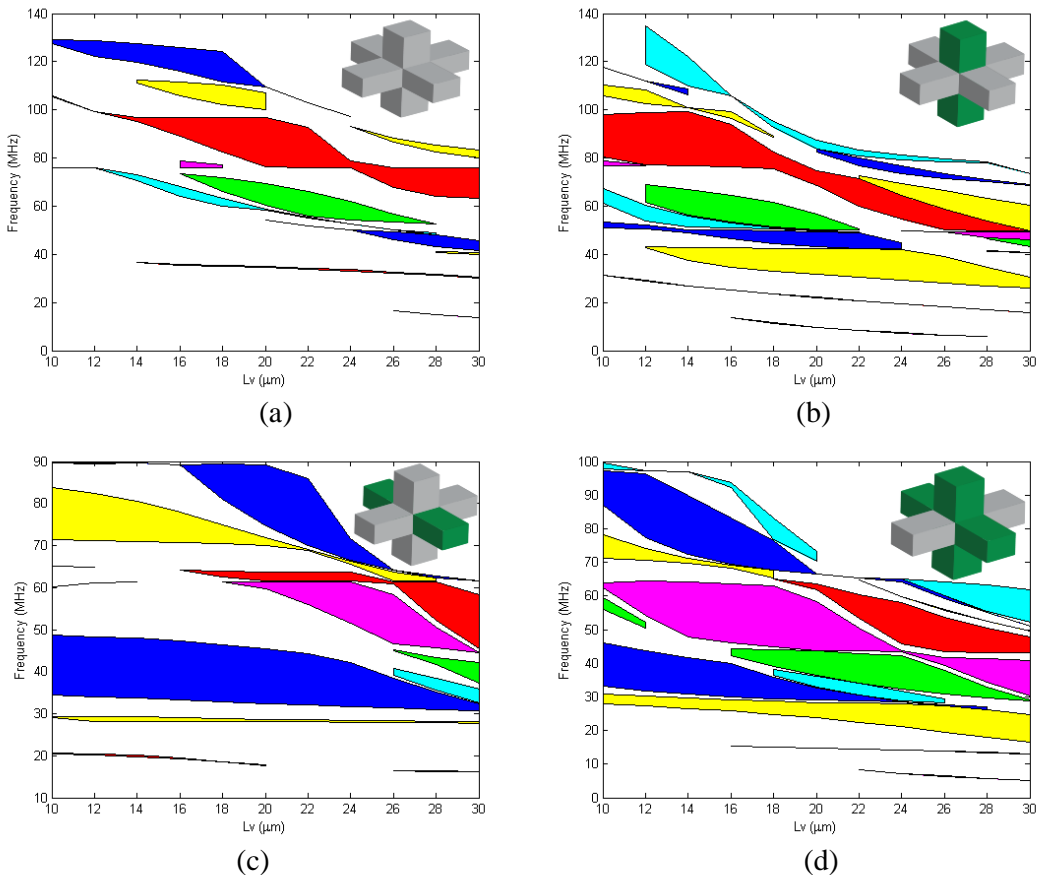


Fig. 5. Dependence of the band structure of the proposed PnC strip with (a) silicon stubs, (b) metallic vertical stub, (c) metallic horizontal stub, (d) metallic stubs on the vertical stub length.

μm .

Similarly, we also perform the simulations for the stubs made of W with different arrangements as shown in Fig. 5b-d. The band gap map of the PnC strip with metallic vertical stub is plotted in Fig. 5b. For the band gaps in the lower frequency range (i.e. 35 – 60 MHz), their width and position on the map almost keep unchanging when varying the stub length of from 12 – 28 μm . For the band gaps in the higher frequency range (i.e. 80 - 140 MHz), the position is shifted toward lower frequencies when the stub length increases. Especially, all gaps in these two gap groups always appear very close. Some maximum gaps obtained in this structure are 12.65 MHz at lower gap boundary of 29.17 MHz and L_v of 24 μm and 22.53 MHz at 76.55 MHz and 14 μm .

On the contrary, the number of the gaps appearing in the model with metallic horizontal stub is less than the one with vertical stub, as shown in Fig. 5c. The gaps are densely opened when the stub length become larger (e.g. from 20 - 30 μm). However, these gap are significantly wide, about 14.26 MHz at 34.53 MHz and 10 μm or 15.83 MHz at 70 MHz and 22 μm . In particular, the gap around 40 MHz is almost constant for the L_v variation.

The last type of the stub which is combined both metallic horizontal and vertical stubs has the band structure as plotted in Fig. 5d. Most gaps occur in lower frequency range and have close gap edges. For example, a 8.2 MHz gap exists at the lower gap boundary of 16.5 MHz for L_v of 30 μm or another 18.88 MHz gap also occurs at 77.45 MHz for L_v of 14 μm .

In summary, one can see from the discussion and graphs in sections 3.2, 3.3 and 3.4 that the proposed PnC structures demonstrate great advantages in generating low and wide band gaps compared with the conventional structures. The gaps of the proposed PnC strip can be flexibly optimized and positioned through two horizontal and vertical stubs. Hence, the side dimensions of the structure can be reduced so that the form factor can be small. With the same stub length variation, the number, width and position of the gaps of the proposed model are more predominating than the classical model. The close gaps in the proposed PnC strip can be seen as a larger equivalent gap. The combination of horizontal and vertical stubs can flexibly open the band gaps.

The number of the gaps of the structures with metallic stub is more significant than the one with silicon stubs. They almost continuously occupy in a certain frequency range of the map gap. The gaps of

these structures are wider than the one with silicon stubs. Compared with silicon stubs, the band gaps can be obtained in lower frequency ranges using metallic stubs.

4. CONCLUSION

Through finite element analysis in COMSOL, the design and simulation of the new PnC strip structures which composed of horizontal and vertical stubs made of tungsten and silicon were presented in this paper. The band gap map is studied and compared among four types of material based stub arrangements. Besides, wide and low characteristics of the band gap of the proposed model significantly increase compared with the conventional counterparts. By varying the length of horizontal and vertical stubs as well as material schemes, the width and position of the band gaps in the band gap map can be optimized to obtain large values at low frequency range. By introducing a new PnC strip structure with two stubs and alternative material arrangement, low and wide acoustic gaps were generated. Our proposed model provides the way towards efficient support tether structures for low frequency MEMS resonators.

Acknowledgments

This work was supported by the National Natural Science Foundation of China and the China Academy of Engineering Physics (U1430102).

REFERENCES

- [1] Ma, C.; Guo, J.; Liu, Y. (2015): Extending and lowering band gaps in one-dimensional phononic crystal strip with pillars and holes. *Journal of Physics and Chemistry of Solids*, **87**, pp. 95-103.
- [2] Pourabolghasem, R.; Khelif, A.; Eftekhar, A. A.; Mohammadi, S.; Adibi, A. (2012): Phononic bandgaps in silicon plate with metallic pillars. *Electronics Letters*, pp. 1147-1148.
- [3] Ma, C.; Guo, J.; Liu, Y. (2015): Simultaneous high-Q confinement and selective direct piezoelectric excitation of flexural and extensional lateral vibrations in a silicon phononic crystal slab resonator. *Journal of Physics and Chemistry of Solids*, **1**(2), pp. 95-103.
- [4] Hsu, F.; Huang, T.; Wang, C.; Chang, P.; Hsu, J. (2012): Phononic crystal strip for engineering micromechanical resonators. *Optoelectronics and Communications*.
- [5] Mohammadi, S.; Eftekhar, A. A.; Pourabolghasem, R.; Mohammadi, S.; Adibi, A. (2011): Phononic bandgaps in silicon plate with metallic pillars. *Sensors and Actuators A: Physical*, pp. 524–530.
- [6] McSkimin, H. J. (1953): Measurement of Elastic Constants at Low Temperatures by Means of

Ultrasonic Waves-Data for Silicon and Germanium. Journal of Applied Physics.

- [7] Khelif, A.; Aubiza, B.; Mohammadi, S.; Adibi, A.; Laude, V. (1975): Elastic constants of tungsten-rhenium alloys from 77 to 298 °K. Journal of Applied Physics, pp. 1526 - 1530.
- [8] Ayres, R. A.; Shannette, G. W.; Stein, D. F (2006): Complete band gaps in two-dimensional phononic crystal slab, Physical Review.